PNAS

Supporting Information for

HPV16 E6 induces chromosomal instability due to polar chromosomes caused by E6AP-dependent degradation of the mitotic kinesin CENP-E

Pippa F. Cosper[†], Laura C. F. Hrycyniak[†], Maha Paracha, Denis L. Lee, Jun Wan, Kathryn Jones, Sophie A. Bice, Kwangok Nickel, Samyuckta Mallick, Alison Taylor, Randall J. Kimple, Paul F. Lambert, and Beth A. Weaver

[†]equal contribution

Corresponding author: Beth A. Weaver

Email: baweaver@wisc.edu

This PDF file includes:

Figures S1 to S8
Table S1

Other supporting materials for this manuscript include the following:

Dataset S1

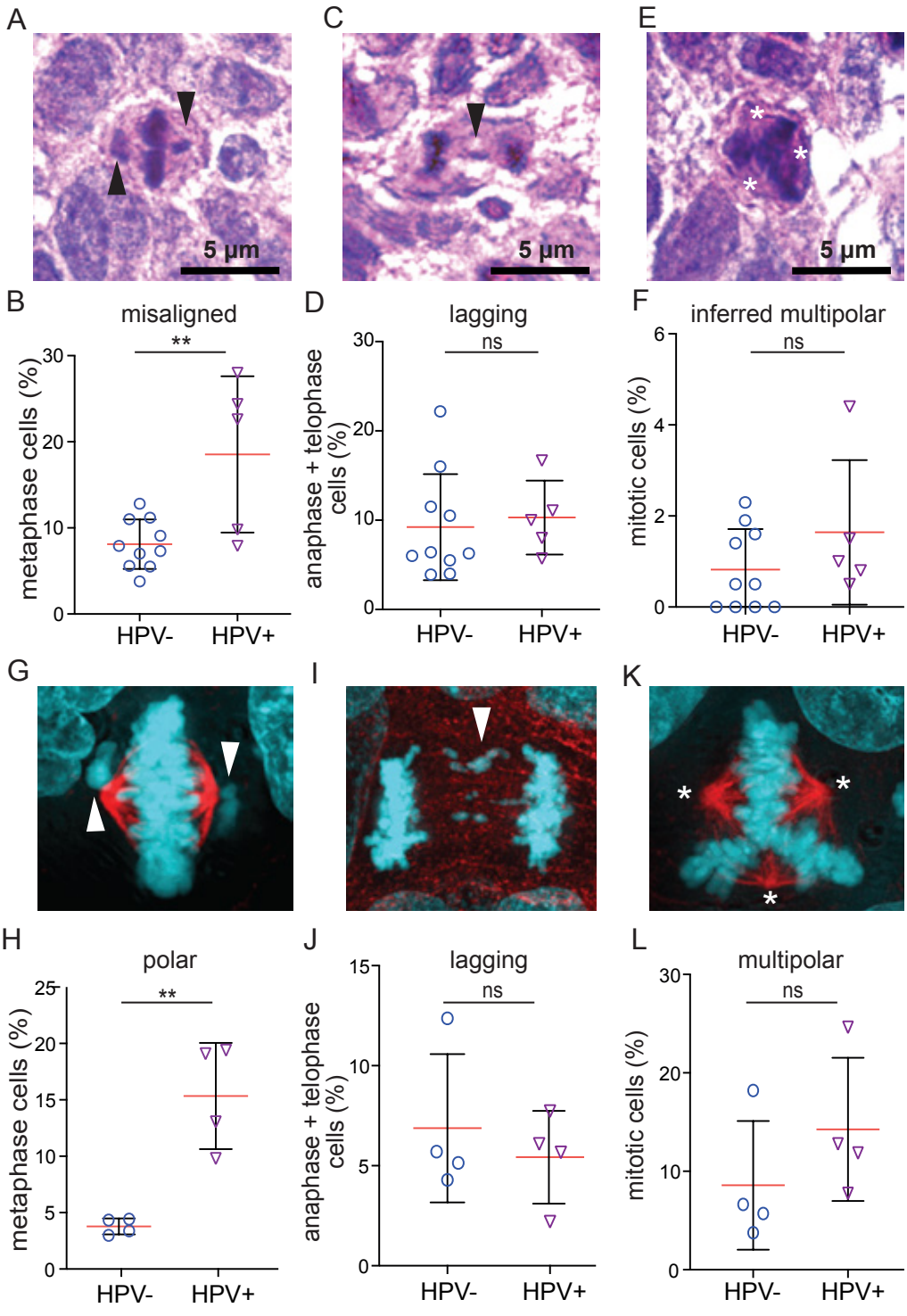

Figure S1. Misaligned chromosomes are enriched in HPV$^+$ HNC PDX tumors and cell lines. (A-F) HPV+ HNC PDX tumors show a specific increase in chromosome congression defects when compared to HPV- HNC PDX tumors. (A) HPV+ mitotic cell with misaligned chromosomes (arrowheads). (B) Quantitation of misaligned chromosomes in HNC PDX tumors. n≥40 metaphases from each of 10 HPV- and 5

HPV+ PDX. (C-D) HPV does not affect incidence of lagging chromosomes. (C) HPV+ HNC PDX cell with a lagging chromosome (arrowhead). (D) Quantitation of lagging chromosomes in HNC PDX tumors. n≥25 anaphase + telophase cells from each of 10 HPV- and 5 HPV+ PDX tumors. (E-F) HPV infection does not affect the incidence of spindle multipolarity in PDX tumors. (E) Mitotic PDX cell with an inferred multipolar spindle based on the position of the DNA. Asterisks indicate the expected location of spindle poles. (F) Quantitation of inferred multipolarity. n>95 mitotic cells from each of 10 HPV- and 5 HPV+ PDX. (G-L) HPV-positive HNC cell lines (UPCI SCC-152, UM-SCC-2, UM-SCC-47, 93-VU-147T) have a significantly increased incidence of polar chromosomes compared to HPV- cell lines (FaDu, UM-SCC-1, UM-SCC-6, UM-SCC-22B). (G) UPCI SCC-152 cell with polar chromosomes (arrowheads). (H) Quantitation of polar chromosomes in HNC cell lines. n≥50 metaphase cells from each of 4 independent experiments. (I-J) HPV infection does not affect incidence of lagging chromosomes. (I) HPV- cell with a lagging chromosome (arrowhead). (J) Quantitation of lagging chromosomes in HNC cell lines. n>50 anaphase + telophase cells in each of 4 independent experiments. (K) Multipolar spindle in HPV+ cell. (L) Quantitation of multipolar mitoses. Error bars indicate SD. **p<0.001. ns = not significant.

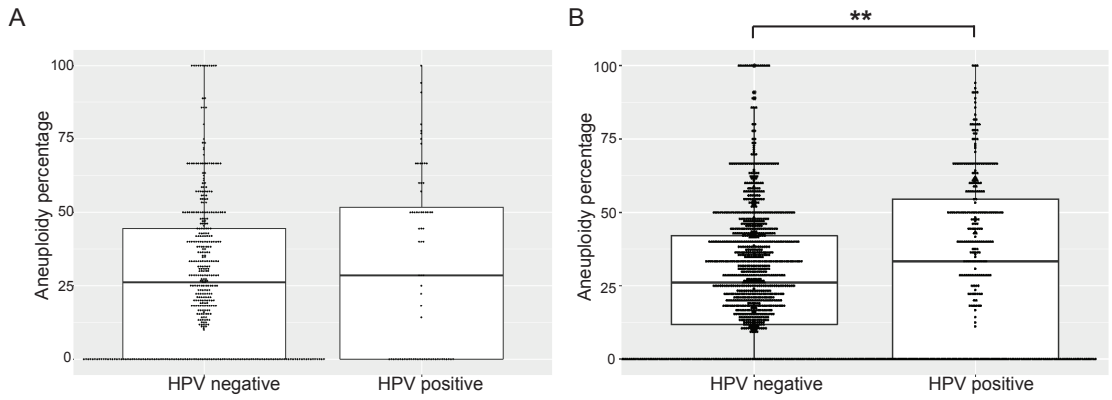

Figure S2. HPV+ SCCs have higher fractions of aneuploidy due to whole chromosome alterations. Aneuploidy alterations due to a whole chromosome event were divided by overall aneuploidy score (number of chromosome arms altered) to calculate percentages (y-axis). Tumors from the TCGA HNC dataset (A) or panSCC (B) are separated by HPV status (x-axis). **p<0.01.

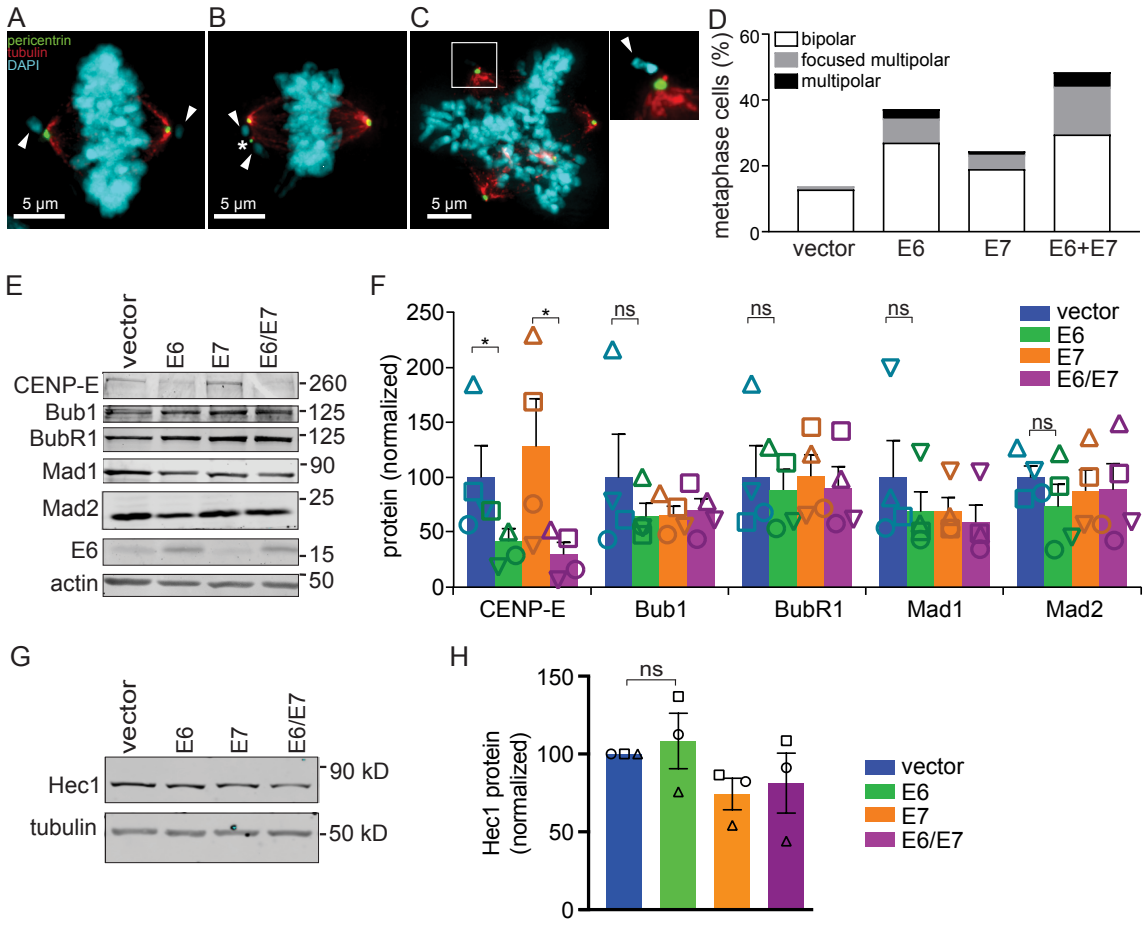

Figure S3. A minority of E6-induced polar chromosomes occur due to multipolar spindle focusing. (A) E6 expressing NOK with 2 polar chromosomes (arrowheads) on a normal bipolar spindle. (B) E6 expressing NOK with 2 polar chromosomes (arrowheads) on a focused multipolar spindle. Extra centrosome indicated with an asterisk. (C) E6 expressing NOK with a polar chromosome (arrowhead in inset) on a multipolar spindle. Inset has brighter DNA signal to better visualize the polar chromosome. (D) Quantitation of the spindle morphologies in NOKs with misaligned chromosomes showing that most misaligned chromosomes occur on normal bipolar spindles. n>45 metaphases from each of ≥3 independent experiments. (E) Expression of E6 alters protein levels of CENP-E, but not other key mitotic regulators. Actin, loading control. (F) Quantitation of protein from n=4 independent experiments. (G) E6 does not alter expression of Hec1, a protein involved in kinetochore-microtubule interactions. (H) Quantification of Hec1 levels from n=3 independent experiments. Shapes indicate which values are from each replicate. Error bars indicate SEM (F) or SD (H). *p<0.05. ns = not significant.

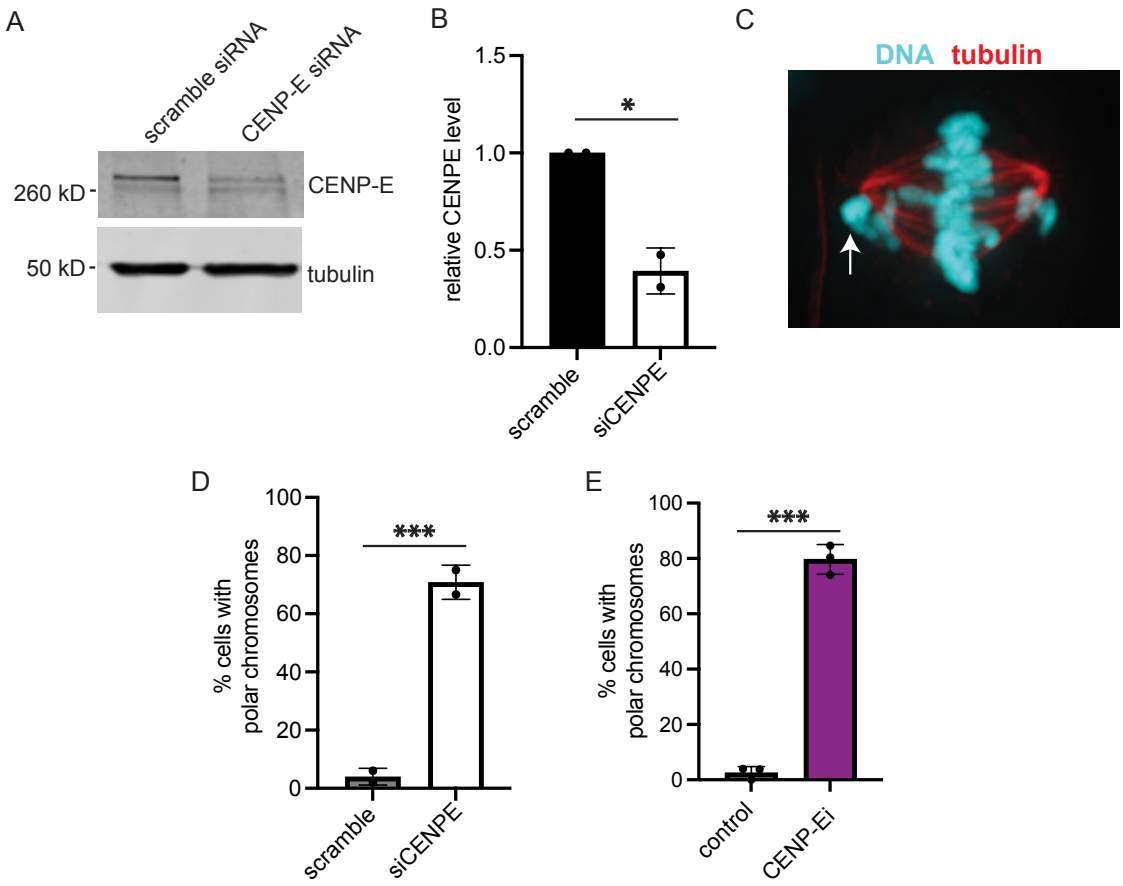

Figure S4. Knockdown or inhibition of CENP-E causes polar chromosomes in NOKs. (A) Immunoblot showing efficient knockdown of CENP-E by siRNA. (B) Quantification of CENP-E protein levels after siRNA. (C) Image of mitotic phenotype induced by CENP-E knockdown. Arrow indicates misaligned chromosome near spindle pole. (D) Quantification of polar chromosomes in LXSN control NOKs 48 hours after transfection of scramble or CENP-E siRNA. n≥50 metaphase cells from each of 2 independent experiments. (E) Quantification of polar chromosomes in LXSN control NOKs after treatment with 0.01 nM of the CENP-E inhibitor GSK923295. n≥50 metaphase cells from each of 3 independent experiments. Error bars indicate SD. *p<0.05. ***p<0.0001.

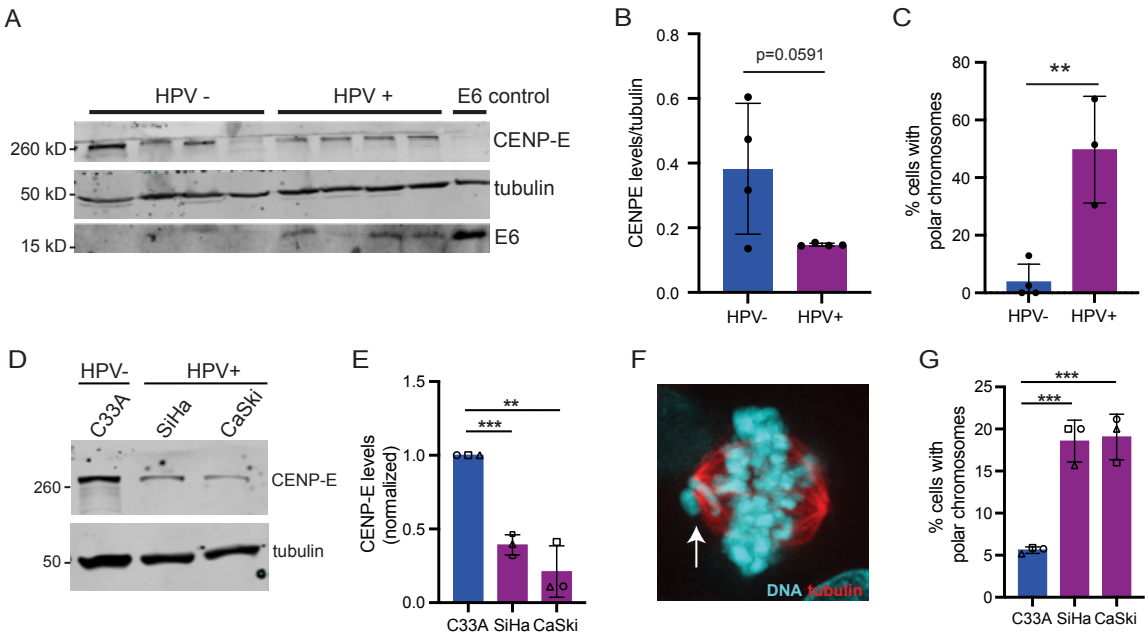

Figure S5. CENP-E protein is reduced in patient HNC tumor tissues and HPV16+ cervical cancer cells and is associated with an increase in polar chromosomes. (A) Immunoblot of patient head and neck tumors (n=4 HPV-, n=4 HPV16+) revealing that the HPV+ tumors typically have E6 expression and decreased CENP-E levels. (B) Quantification of CENP-E protein normalized to tubulin for each tumor (n=4 per group). (C) Quantification of polar chromosomes in the HPV- and HPV+ tumors shown in (A) and (B). One of the HPV+ tumors did not have an adequate number of mitotic cells for accurate quantitation. A median of 25 cells in metaphase were counted for each sample. (D) Immunoblot showing reduced CENP-E levels in the HPV16+ cervical cancer cell lines SiHa and CaSki compared to the HPV- cervical cancer cell line C33A. (E) Quantification of CENP-E protein normalized to tubulin. n=3 independent experiments. (F) Representative image of a polar chromosome (arrow) in SiHa cells. (G) Quantification of polar chromosomes in cervical cancer cells. n≥ 50 metaphase cells from each of 3 independent experiments. Error bars indicate SD. **p<0.01, ***p<0.0001.

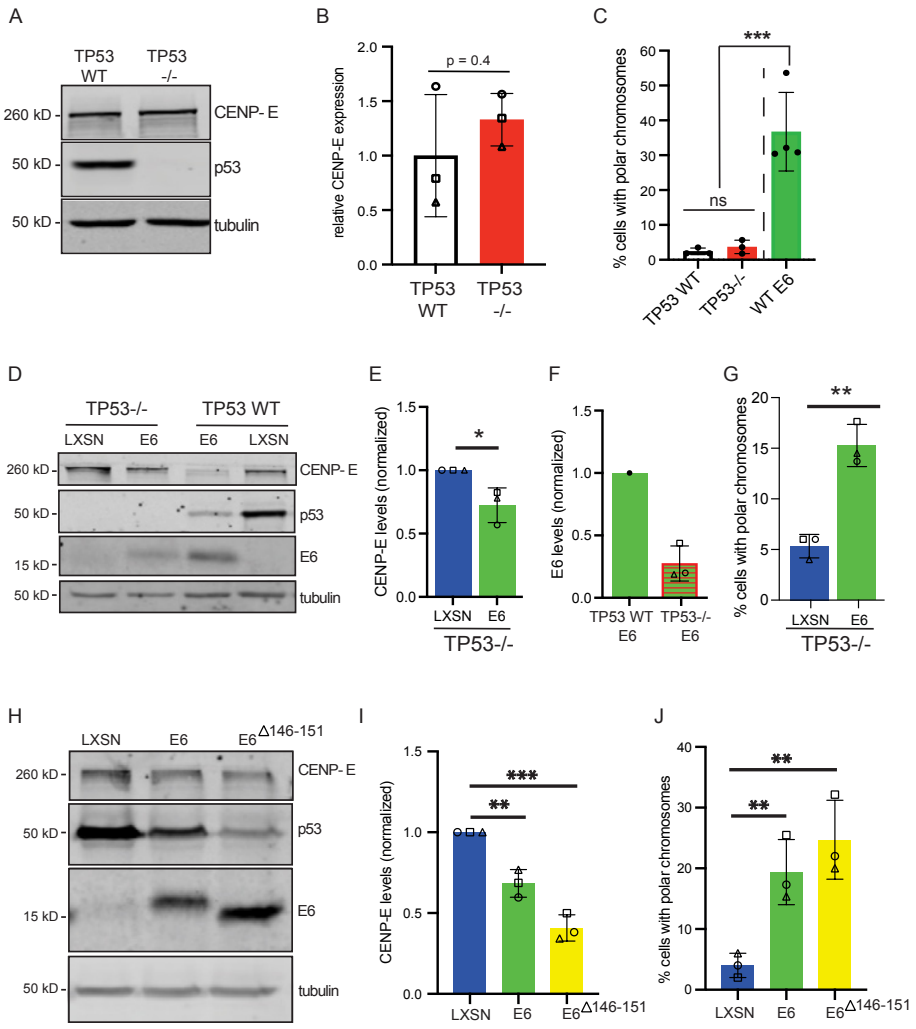

Figure S6. E6-induced decrease in CENP-E levels and resulting polar chromosomes are independent of p53 and the E6 PDZ binding domain. A) Immunoblot showing that loss of p53 in NOKs does not affect CENP-E protein levels. B) Quantification of A. n = 3 independent experiments. C) Loss of p53 does not induce polar chromosomes in NOKs. Effect of HPV16 E6 on polar chromosomes in NOKs is shown for comparison. (D) Immunoblot showing that CENP-E levels are reduced in TP53-/- NOKs that express E6. (E) Quantification of CENP-E protein level normalized to tubulin in LXSN- or E6-expressing TP53-/- NOKs. n=3 independent experiments. (F) Quantification of E6 protein levels in the TP53 WT NOKs used in the majority of this study and in TP53-/- NOKs. The level of E6 in the TP53-/- NOKs is only ~25% the level TP53 WT NOKs. (G) Quantification of polar chromosomes in LXSN- or E6-expressing TP53-/- NOKs. n≥ 50 metaphase cells from each of 3 independent experiments. (H) Immunoblot showing that the $E6^{\Delta 146-151}$ mutant, which lacks a PDZ binding domain, still causes a decrease in CENP-E levels, as well as the decrease in p53 that has been previously described. (I) Quantification of CENP-E protein level normalized to tubulin. n=3 independent experiments. (J) Quantification of polar chromosomes in LXSN-, E6, or $E6^{\Delta 146-151}$-expressing NOKs. n≥ 50 metaphase cells from each of 3 independent experiments. Shapes indicate which values are from each replicate. Error bars indicate SD. *p<0.05. **p<0.01. ***p<0.0001. ns = not significant.

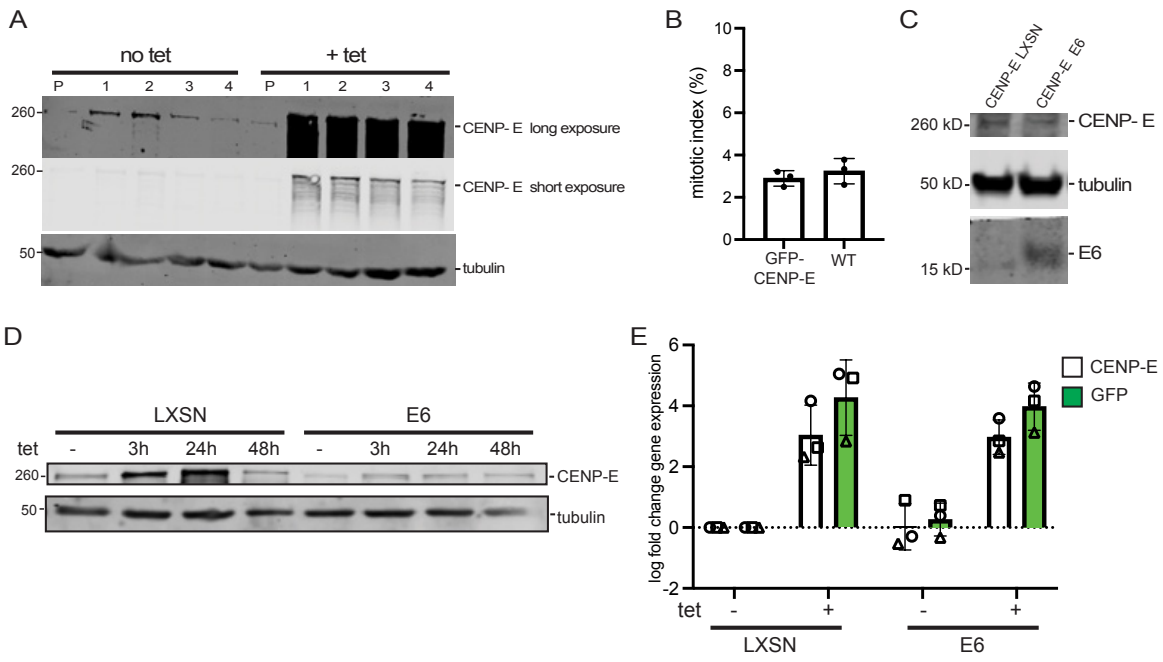

Figure S7. Characterization of tet-inducible GFP-CENP-E NOKs. A) CENP-E protein expression increases upon tetracycline (tet) induction in four GFP-CENP-E subclones but not the parental (P) cell line. Subclone #4 was selected for further experiments. B) Expression of GFP-CENP-E does not affect mitotic index. (C) Immunoblot showing selective expression of HPV16 E6 after subclone 4 was transduced with retrovirus containing an LXSN control vector or HPV16 E6. D) Time-course of CENP-E expression after tet induction in LXSN or E6 expressing GFP-CENP-E NOKs. E) qRT-PCR for GFP and CENP-E mRNA reveals equivalent increases in GFP and CENP-E gene expression after tet induction in both LXSN and E6-expressing GFP-CENP-E NOKs.

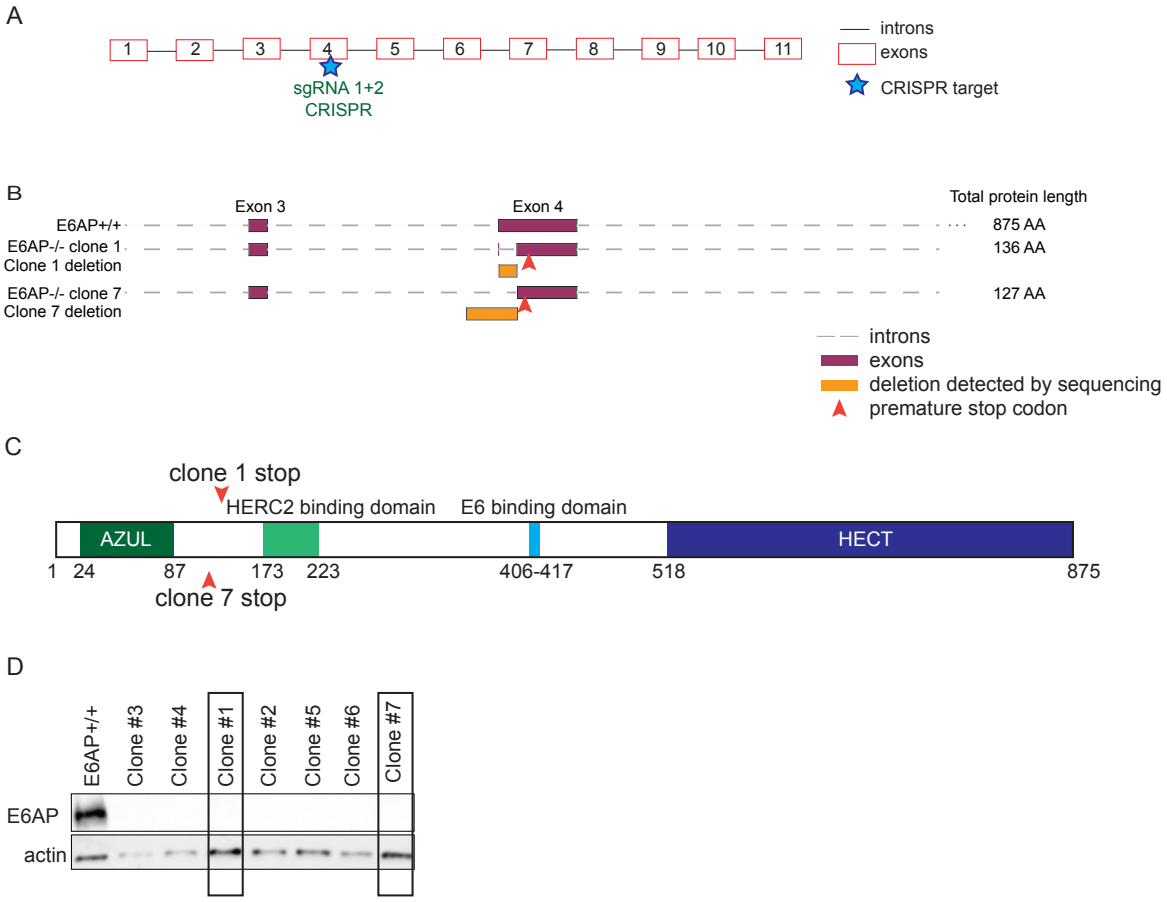

Figure S8. Generation of E6AP-/- NOKs. A) Schematic of E6AP (UBE3A) gene showing location of CRISPR targeting. B) Edits in clones 1 and 7. C) Schematic of E6AP protein showing relevant domains. Asterisks indicate location of premature stop codons introduced by CRISPR editing for both E6AP-/- clones used. Note that the E6AP-/- clones would not produce a protein with E6-binding or ubiquitin ligase domains. D) Immunoblot showing that E6AP-/- clones #1 and #7 have no E6AP protein expression. Actin, loading control.

Table S1. Primers used in qRT-PCR

Primer	primer name from Weng et al (84)	sequence 5'-->3'
CENP-E qPCR exon 18 F	NA	actcagttcaaaagtagagctgc
CENP-E qPCR exon 19 R	NA	tcaagggctacagtttcagca
CENP-E qPCR exon 8 F[#]	1	gaaagcagagagaagggtgaa
CENP-E qPCR exon 9 R	2	tcactgcctgcaagatcaac
CENP-E qPCR intron 8 R	3	tgttttggcccatacagtaca
CENP-E qPCR exon 3 F	13	aaatagcagcaccaatcatcg
CENP-E qPCR intron 3 R	15	gcacagacgcccaagacta
CENP-E qPCR exon 7 F	17	gcaggcattatggagaaaca
CENP-E qPCR intron 7 R	19	aaaaggcaagctgtagaaaaa
GFP F	NA	ggagcggacgatcttcttca
GFP R	NA	agggtgtcgccctcgaa

[#]Primer used for both exon-exon amplification with exon 9 R and exon-intron amplification with intron 8 R. NA, not applicable.

Dataset S1.xls (separate file). Source data.